Environment and Climate Protection (2022)
Clausius Scientific Press, Canada

DOI: 10.23977/envcp.2022.010102
ISSN 2523-6504 Vol. 1 Num. 1

# *Application of Multiple Detection Data in the Impact Analysis of Typhoon Lionrock*

**Chenxiao Shi[1,2], Chunhua Wang[3,*], Jianhua Du[1,2]**

*[1]Hainan Province Meteorological Information Center, Haikou, Hainan, 57020, China*
*[2]Key Laboratory of South China Sea Meteorological Disaster Prevention and Mitigation, Haikou, Hainan, 570203, China*
*[3]Qionghai City Meteorological Bureau, Qiongha, Hainan, 571400, China*
*[*]Corresponding author*

***Keywords:*** Multiple Detection Data, Rainfall, Gale, Analysis, Application

***Abstract:*** This research analyzes the rainfall and wind process of Typhoon Lionrock by integrating conventional and unconventional detection data. The results indicate that: 1) Typhoon Lionrock was generated offshore, during which water vapor replenished and cold air moved continuously southward, bringing a large storm to Hainan Island and the southern and western regions of Guangdong; 2) The combination of vertical velocity of the wind profiler radar and PWV, TBB can accurately show the cloud and rain occurrence region and anticipate the development, occurrence, and termination of typhoon precipitation; it also correlates well with the intensity of precipitation. 3) The horizontal wind field of wind profiler radar and the MTCSWA wind field map can accurately reflect the movement process of typhoons, and areas with strong winds; 4) The analysis based on satellite cloud map and radar data revealed that the overall structure of Typhoon Lionrock is loose, which can be further analyzed in conjunction with other observation data.

## 1. Introduction

In addition to conventional observation means such as automatic stations, the modern detection means of meteorology have developed non-conventional observation means such as GPS/MET precipitable, wind profiler radar, Doppler radar, and multi-source data products based on different detection means[1]. Numerous academics from both China and overseas have examined and evaluated numerous weather processes based on unconventional information and data products, achieving improved application outcomes[2-5]. Liu, S. Y. [6] used the Hong Kong Observatory's wind profiler radar data to identify the mesoscale phenomena of the southwest monsoon and planetary boundary layer associated with heavy precipitation and demonstrated that changes in the wind profiler radar wind field are predictive of the onset of heavy precipitation. Zhou, X. Y.[7] and Gou, A. N.[8] determined, using wind profiler radar, that wind profiler radar can reveal the small structural changes of horizontal motion in the vertical direction. The wind profiler radar has excellent spatial and temporal resolution and can display the interaction between Taiwan's core mountain range and complicated topography and the typhoon wind field in all its granularity[9]. Guo, J. F.[10-11] and Chen, X. L.[12] analyzed the characteristics of GPS precipitable water in different regions and different

rainfall processes, concluding that GPS/MET information has significant indication significance in rainfall, strong convective weather, and artificial rainfall operation. Pan, W. H.[13] examined ground-based GPS atmospheric precipitable water information from 2010 to 2019 in Fujian Province and discovered that the accuracy of ground-based GPS atmospheric precipitable water in Fujian is greater than that of ERA-Interim reanalysis information. Small- and medium-scale convective storms' internal structure, occurrence and development mechanism, and evolution features may also be shown by weather radar echo maps[14-15]. Ren, X. Y. et al[16] and Diao, X. G. et al[17] used Doppler weather radar data to analyze the environmental physical quantities and structural characteristics of storm intensity produced by typhoons, comparing the characteristics of small-scale cyclonic vortices that induced and did not induce tornadoes, and discovered that the unstable structure of upper-layer dry air and lower-layer humid air, upper-layer humidity with thick humid layer, strong lower-layer vertical wind shear and large relative storm helicity are the key physical quantities and factors that induce tornadoes. Chen, Z. G.[18] conducted a comparative analysis of tornadoes derived from the periphery of two typhoons using Doppler weather radar data in Guangzhou, and discovered super monolithic characteristics in radar reflectivity, with the strongest reflectivity above 59 dBZ, and obvious velocity pairs in both low elevation angles. He, F. S.[19] observed that short-term intense precipitation was manifested on the Doppler radar radial velocity map as upwind zone, extensive convergence zone, and gale zone, with the upwind zone type being the most noticeable in a large number of levels; it was primarily manifested as a block on the echoes. The methodology, when combined with MTCSWA wind field data[20], may better represent the horizontal wind field structure of TC and describe the intensity features of strong TC[21]. Xiang, C. Y.[22] examined MTCSWA wind field data in the East China Sea area and discovered that TC intensity was inversely related to maximum wind speed radius and positively proportional to wind circle radius at all levels.

In conclusion, many conventional and non-conventional observations and data products can accurately capture the intricacies of wind field and rainfall variations. Typhoon Lionrock made landfalls in Hainan Province in October 2021, generating torrential rainfall, stormy weather, and seawater pouring backward in certain portions of the island, resulting in tens of millions of RMB in economic damages. As a result, this study analyzes the wind and rainfall characteristics of this typhoon in October 2021 from the standpoint of meteorological data, in order to provide some valuable references for future rainfall and wind forecasting and forecasting service refining. Furthermore, GPS/MET water vapor data and MTCSWA wind field data are considered in this paper, which can not only fill research gaps in these two data products on typhoons, rainfall and gale weather processes, and water vapor climate distribution characteristics in Hainan Province, but also provide more possibilities for future rainfall and gale weather forecasting.

## 2. Overview of the Typhoon Process

The location and intensity of Typhoon Lionrock every 6 hours provided by the CMA tropical cyclone best path data set (tcdata.typhoon.gov.cn)[23] (Figure 1) are used in this analysis.

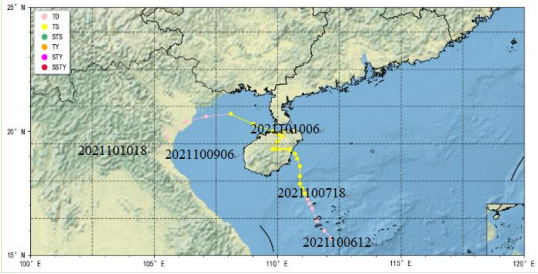


Figure 1: Path of Typhoon Lionrock (No.2117)

At 08:00 on October 6, Typhoon Lionrock formed in the middle South China Sea (15.7 ℃N, 112.2 ℃E) and traveled west-northwest at a pace of roughly 10 kilometers per hour, steadily growing in severity and retaining the tropical storm classification. The typhoon intensified and traveled northwesterly at 05:00 on the 8th in the sea approximately 175 kilometers southeast of Wanning City (17.5 ℃N, 111.1 ℃E), settling at 22:50 on the 8th in Tanmen Town, Qionghai City. After landing, it traveled westward for a short time before abruptly turning north, entering Qiongzhou Strait in the afternoon of September 9th, and then moving westward into the northern sea surface of Beibu Gulf. Typhoon Lionrock made impact off the coast of northern Vietnam around 11:00 a.m. on the 10th. And the numbering came to an end on the 10th at 18:00. From this, Typhoon Lionrock has the characteristics of offshore generation and sluggish movement.

## 2.1 Typhoon Rainfall Situation

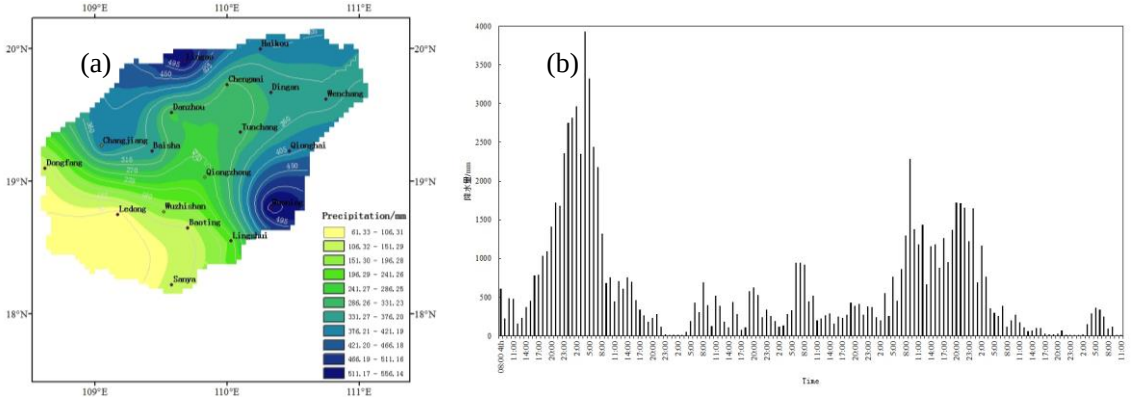


Figure 2: Spatial and temporal distribution of rainfall from 08:00 on October 4 to 11:00 on October 10 (a~b)

The province received significant rain from 08:00 on October 4 to 11:00 on October 10 as a result of Typhoon Lionrock. Around the start of the typhoon, the rainfall peaked at 10:00 on the 5th; as the typhoon moved forward, the rain increased, and the rainfall peaked again on the 8th and 9th (Figure 2(b)). Rainfall regions were mostly concentrated in the northern and eastern sections of Hainan Island, namely between Qionghai and Wanning, as well as along the coast between Haikou and Lingao and Changjiang (Figure 2(a)). This is due to the typhoon's northward folding, which causes rain to fall mostly in the east and west of Hainan Island. Wanning had the highest accumulation of rain, with 570.7 mm, followed by Lingao County, which had 544.4 mm.

## 2.2 Weather Condition

The subtropical high pressure was rising unusually northward at 500hpa (Figure 3 isogram), and the relative humidity was essentially over 90%, which was conducive to the occurrence and development of deep cumulus convection and vertical movement. The wind direction on the typhoon's south side changed from westerly airflow to southwesterly airflow, indicating that the southwesterly airflow on the typhoon's south side was constantly transporting water vapor, combined with the stable blocking effect of the subtropical high pressure on the north side and the cold air constantly moving southward. As a result, there was an obvious airflow convergence near Typhoon Lionrock, as well as strong radiation of airflow outflows from high altitude (Figure omitted), which was conducive to upward movement, prompting the development of the typhoon's peripheral cloud system and wrapping more water vapor to the north. When combined with Figure 4 water vapor flux, the water vapor convergence center from the western South China Sea over the

sea gradually expanded to the north, water vapor intensity gradually increased, and at 20:00 on the 8th, there were two water vapor convergence centers, located in Hainan Island and southern Guangdong to western Guangdong area. This is consistent with the actual situation, at 20:00 on the 8th Hainan Island and the southern and western coastal areas of Guangdong appeared strong rainfall process.

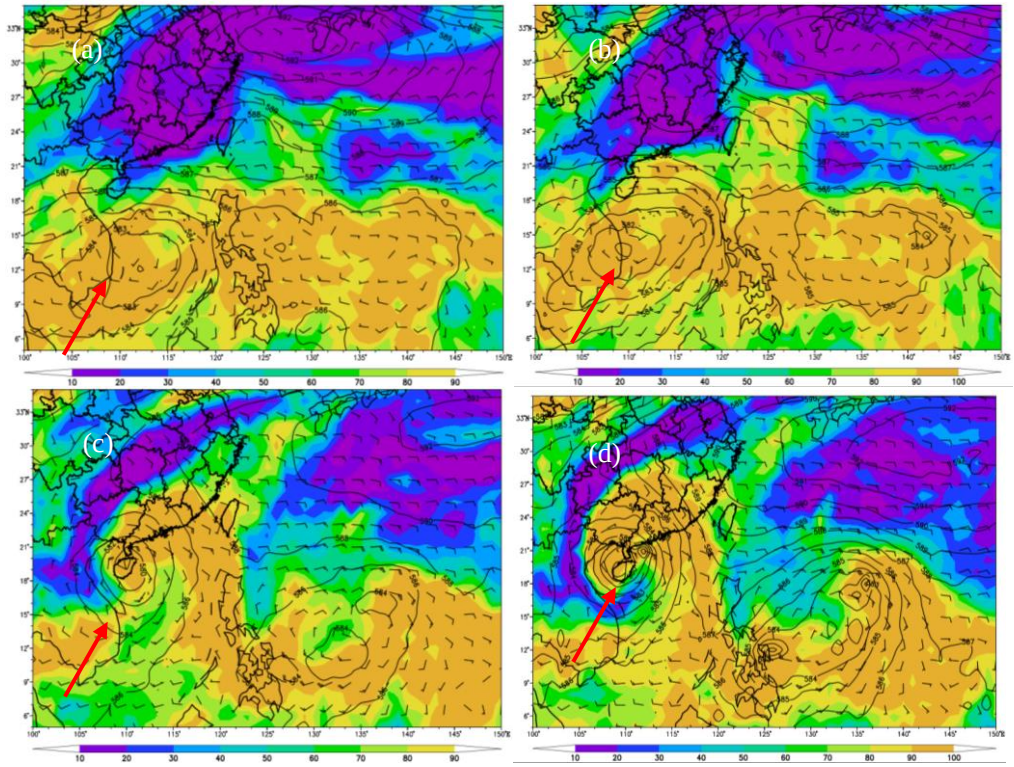


Figure 3: 500hpa height field (isogram), relative humidity (color spot) superimposed on 925hpa wind field at 08:00 (a), 20:00 (b), 20:00 (c) and 08:00 (d) on October 6, 2021

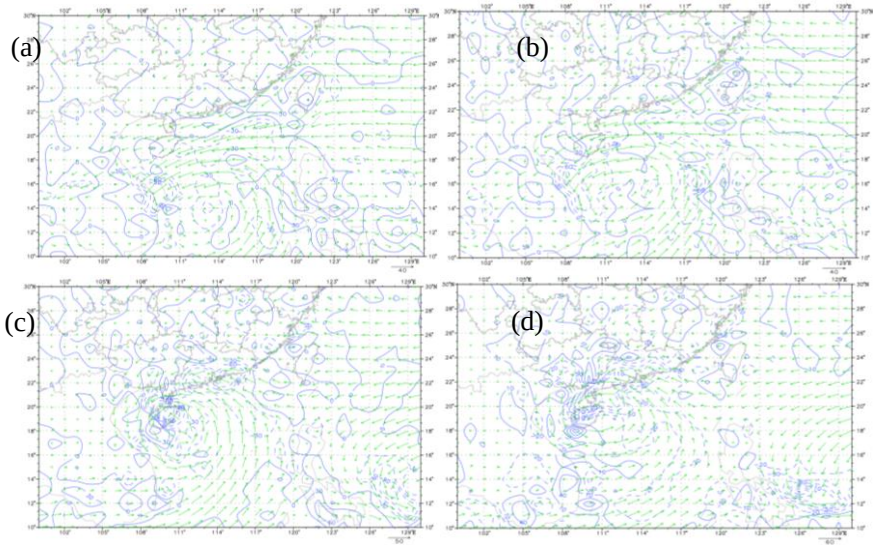


Figure 4: Convergence and divergence of water vapor flux at 08:00 (a), 20:00 (b), 20:00 (c), and 08:00 (d) on 6, 8, and 9 October 2021

Satellite cloud data suggests that there is a huge region of tropical convective clouds in the middle South China Sea at the start of the tropical depression, with noticeable spiral structure,

although the cloud structure is somewhat loose. From the evening of the 7th until the morning of the 8th, a comma-shaped cloud mass with heavy convection appeared around the center of Typhoon Lionrock, suggesting that the typhoon's strength had increased. These clouds revolved cyclically around the center, with an uneven structure (figure omitted). Because TBB can accurately reflect the strength of convection and reveal the presence of clouds as well as some salient features of clouds at various stages of evolution[24-25], the FY-2G infrared cloud top brightness temperature TBB map (Figure 5) reveals a large area of low TBB values in the central South China Sea and the ocean surface east of the Philippines. The two low value zones went northward or northwestward while Typhoon Lionrock advanced northward or northwestward, with the TBB value on the ocean surface east of the Philippines reaching as low as 180 K. By 20:00 on the 8th, the TBB value across Hainan Island, southern Guangdong, and western Guangdong had declined from 252.8 K to below 228.5 K, suggesting a vast area covered by clouds and rain and intense convective activity of cloud masses (Figure 5(e)). Combining the above measured data and weather condition analysis, it can be seen that Typhoon Lionrock continued to absorb and carry a large amount of water vapor to the north as it moved northward, and this, combined with the presence of cold air continuously moving southward, caused a large-scale intense rainfall process, and two areas of intense rainfall appeared, which were located on Hainan Island and the southern and western coastal areas. This is consistent with the study of rainfall intensity and heavy rainfall fall locations shown above.

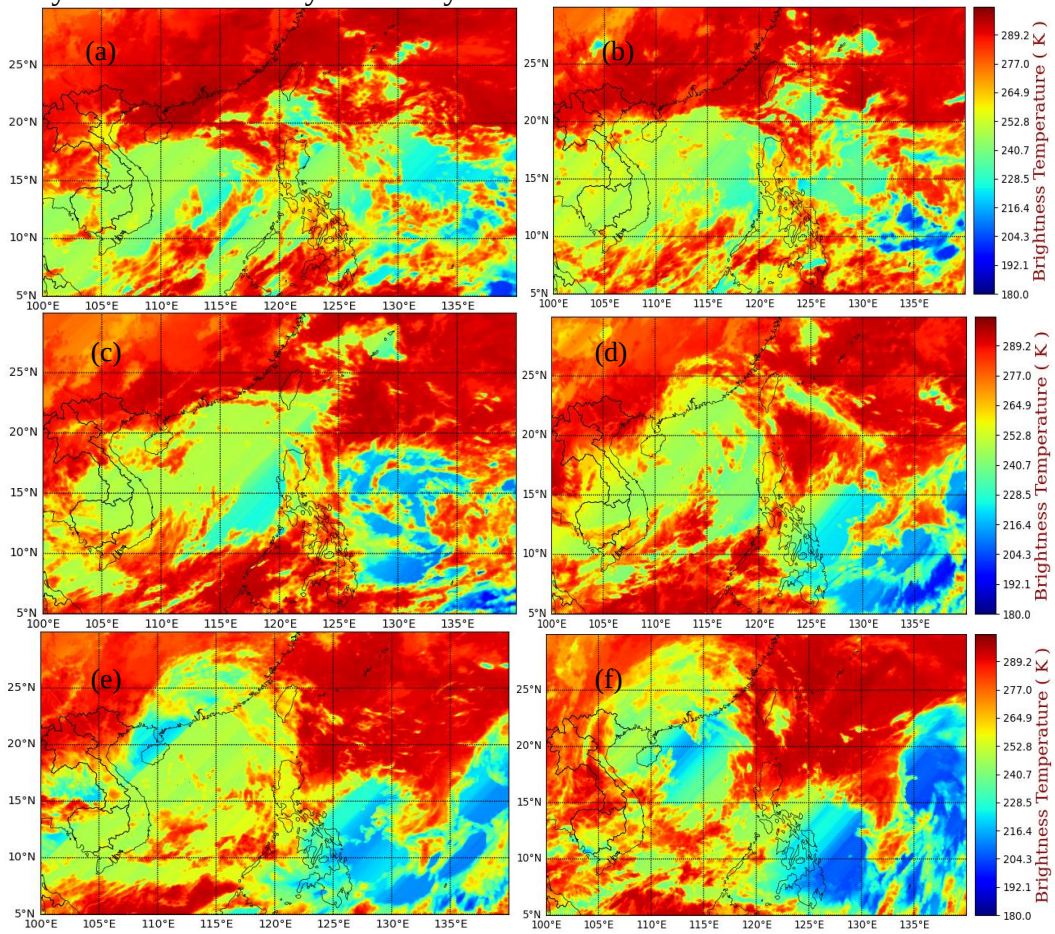


Figure 5: FY-2G infrared cloud top brightness temperature (TBB) diagrams at 08:00 (a) on 06 October, 20:00 (b) on 06 October, 08:00 (c) on 07 October, 08:00 (d) on 08 October, 20:00 (e) on 08 October, and 08:00 (f) on 09 October, 2021

## 3. GPS/MET Precipitable Water Volume (PWV) Analysis

GPS/MET can detect actual water vapor content in the air column, which is closer to water vapor density and, unlike relative humidity, which is temperature dependent, is not temperature restricted [1,26]. In general, the peak PWV correlates to a rainfall peak, which serves as a reference for analyzing rainfall meteorological processes. However, there are cases where a PWV peak occurs without rainfall, which is due to the fact that water vapor conditions are a necessary but not sufficient condition for the rainfall process, and rainfall will not occur if there is no trigger mechanism and unstable stratification[26].

Figure 6 depicts the progression of PWV and station rainfall over time during Typhoon Lionrock at Danzhou, Qionghai, Wuzhishan, and Sanya stations. Figure 6 shows that, prior to the landfall of Typhoon Lionrock, the typhoon peripheral cloud system had covered Hainan Island (Figure omitted), and that, combined with the influence of the easterly airflow, the PWV values of the four stations on the island had been fluctuating upward since 8:00 on the 4th; that is to say, energy accumulated above the atmospheric column, and the PWV value had been maintained at more than 60 mm. The PWV value fell at 16:00 on the 5th, when the unstable energy across the air column was released. When combined with the actual precipitation occurrence, the precipitation at Qionghai station decreased, and there was little or no precipitation at Danzhou, Wuzhishan, and Sanya stations. Rainfall from Typhoon Lionrock continued to affect Hainan Island until the typhoon made landfall; precipitation continued to fall, and the PWV value at each station fluctuated to stay above 60 mm. The impact of rainfall had ended by the end of the typhoon, and the PWV values had returned to below 60 mm.

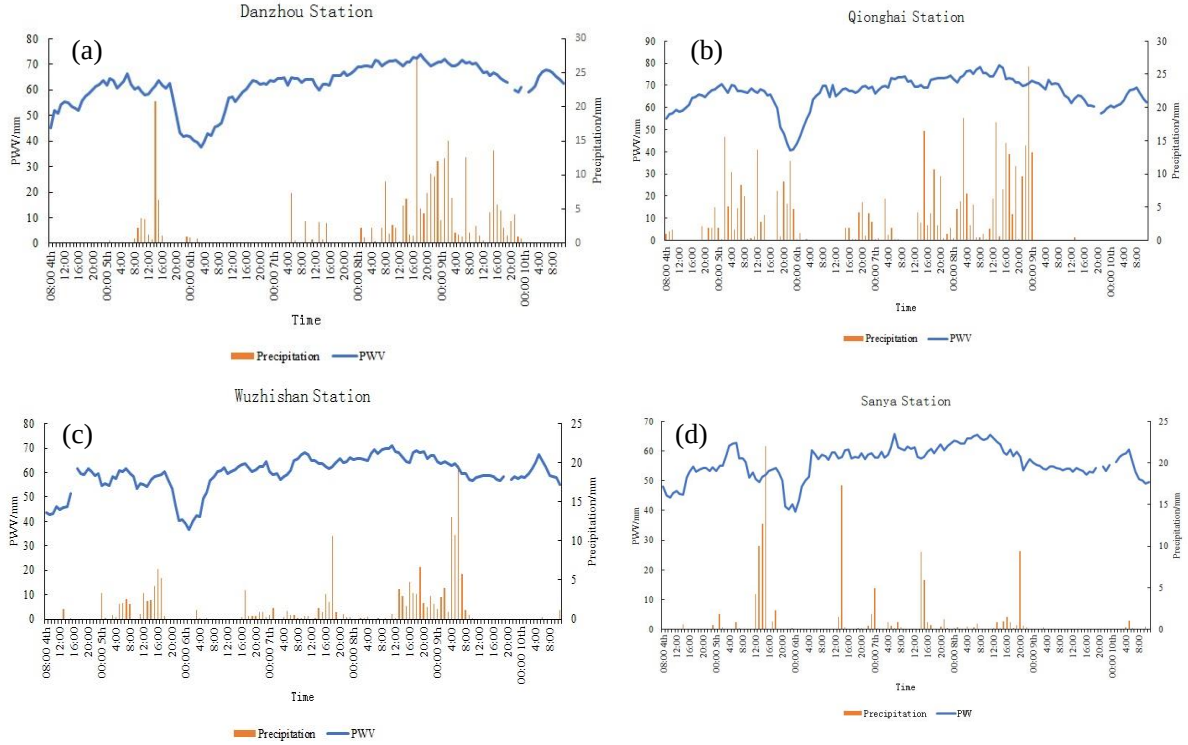


Figure 6: Evolution of precipitation and GPS/MET PWV at Danzhou (a), Qionghai (b), Wuzhishan (c) and Sanya (d) stations during the Typhoon Lionrock

## 4. Analysis of Wind Profiler Radar Data

Wind profiler radar recorded wind direction and wind speed information, which is more

comprehensive and rich in terms of geographical and temporal distribution than standard detection data[27]. The wind profiler radar of Haikou (110.36 °E, 20.00 °N) is used in this study to examine the wind field characteristics of the height layer during two typhoons by utilizing the entire layer horizontal wind field continually captured by this radar and the vertical velocity derived by the method.

### 4.1 Changes of Horizontal Wind Field

Figure 7(a) shows that before 14:00(UTC) on the 8th, the entire layer of horizontal wind field was dominated by partial northeast winds, and the Haikou wind profiler radar was located in the northwest direction of the typhoon, indicating that Typhoon Lionrock was gradually moving westward and approaching the eastern coast of Hainan Island. Its outer wind circle has started to cover the majority of Hainan Island, and the wind speed has reached 20 meters per second. From 14:00 (UTC) to 15:00 (UTC), the wind direction shifted counterclockwise from easterly to northeasterly at an altitude of about 7000m, and counterclockwise from easterly to northwesterly at an altitude of about 6000m with height (red box in Figure 7(a)), indicating that the typhoon landed on Hainan Island at this time; the horizontal wind direction at the near surface layer also changed from easterly to northeasterly. The horizontal wind direction above 1 km height gradually changed from northeasterly to southeasterly after 14:00 UTC. The wind speed in the entire layer decreased as the typhoon made landfall, especially in the near-surface layer, where it was only 4m/s.

When combined with Fig. 7(b), it is discovered that on the 9th, from 01:00(UTC) to 03:00(UTC), the entire layer is basically dominated by the southeasterly wind, except for the near-surface layer, where the wind speed increased and then gradually decreased, while the wind speed at the rest of the height remained constant, essentially around 16m/s. The wind direction in the near-surface layer gradually changed from easterly to southeasterly from 03:00 (UTC) to 06:00 (UTC), while at other heights it gradually changed from southeasterly to easterly, and the wind speed was low at 03:30 (UTC) and then gradually rose. The wind direction in the near-surface layer shifted from southeasterly to easterly, then counterclockwise to westerly to southwesterly between 06:30 and 11:00 UTC. The wind direction above 1km shifted from southeasterly to southerly, and the wind speed was low, ranging from 2-6m/s, suggesting that the typhoon center had traveled northward and was already at Haikou. The wind speed was higher than that of the typhoon core when it passed over Haikou. The typhoon core had moved westward at this point, and only the peripheral wind on the right side of the typhoon had hit Haikou. At 20:30 (UTC), the wind direction shifted from southwesterly to southeasterly, and the wind speed decreased (Figure 7(c)), as the Typhoon Lionrock moved away from Haikou, which is consistent with the findings of Shi, C. X. et al[28].

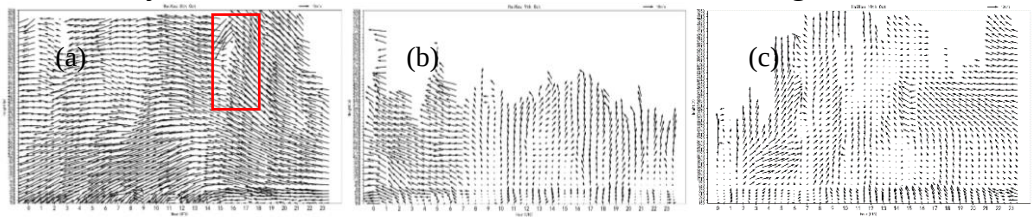


Figure 7: Variation of horizontal wind field of wind profile at Haikou station from October 8 to 10 (UTC; (a)~(c))

### 4.2 Changes of Vertical Velocity

The vertical velocity detected by wind profiler radar can indicate the occurrence and intensity of rainfall[28]. Vertical velocity is positive when downward, i.e., sinking air, and negative when upward,

i.e., rising air, according to the wind profiler radar industry standard(QX/T 629-2021). According to Figure 8(a), the vertical velocity of the entire level height on the 8th day was basically between -0.0 and 9.0m/s, except for the positive values of vertical velocity at 06:00(UTC) and 19:00(UTC)-19:30(UTC) near the ground level, especially for the height below 5000m, where the vertical velocity reached between -7.5 and 9.0m/s at 07:00(UTC)-14:30(UTC). Combined with the actual conditions, not only the rainfall continued to occur within this period, but also the rain intensity was large. By 10:00 on the 9th (UTC), the vertical velocity was between -0.8 and 0.8m/s. Combined with the actual conditions, the rainfall ended after 18:00 on the 9th. Only on the 10th 07:00(UTC)-08:30(UTC) the vertical velocity of the whole level height reached between -4.8 and -5.6m/s at one time, especially at 07:00(UTC), and the real situation showed that rainfall occurred on the 10th 15:00-17:00, especially at 15:00, the rainfall amount reached 4.0mm, and the rain was larger than the other two times. After that, the vertical velocity of the whole atmosphere was basically positive, combined with the horizontal wind field on the 10th, the horizontal wind direction in the near-ground level was basically south-south wind gradually turned to southeast wind after 09:00 (UTC), and the horizontal wind direction in the height above the near-ground layer was basically southeast wind turned to east wind, and the wind speed weakened (Figure 7(c)), indicating that Typhoon Lionrock had moved away from Haikou, and the rainfall process brought by it had ended (Figure 8(c)).

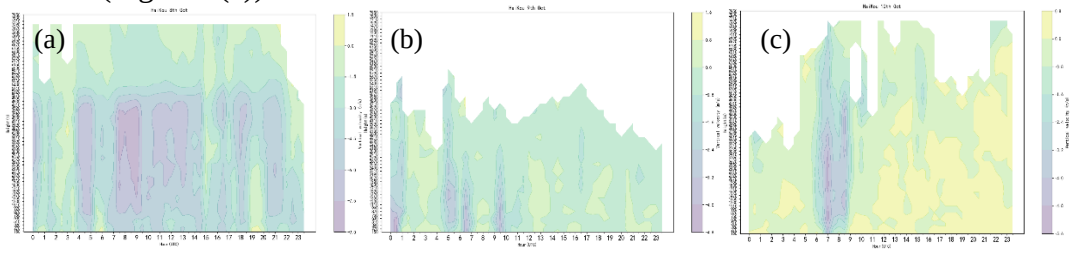


Figure 8: Variation of vertical velocity of wind profile at Haikou station on October 9-10 (UTC; (a)~(c))

In conclusion, the horizontal wind field of wind profiler radar can accurately depict typhoon movement; when the wind direction changed from southeasterly to easterly, the typhoon progressively moved away from the sea entrance. The main difference is that Typhoon Lionrock moved northward while the wind direction was southerly; wind profiler radar is particularly sensitive to the changing of precipitation particles and has a strong relationship to precipitation intensity. When the typhoon's perimeter hit Haikou, the vertical velocity was negative, and when its absolute value reached its maximum, it indicated the most precipitation particles and a high intensity of precipitation. When the typhoon proceeded westward away from Haikou, the incidence of occasional paroxysmal precipitation and the actual precipitation start and finish timings were almost identical.

## 5. Radar Data Analysis

Figure 9(a) shows that at 22:35 on October 8, prior to the landfall of Typhoon Lionrock, the echo reflectivity of most of Hainan Island exceeded 30dBZ, indicating that most of the island experienced rainfall, with moderate to heavy rainfall in the northern and central-western areas of Hainan Island and light rainfall in the surrounding offshore areas. According to the MTCSWA wind field data, before Typhoon Lionrock made landfall, the wind speed was low except for Qionghai and the western part of Hainan Island, but the wind speed was high around most of Hainan Island and the offshore area, especially in the northeastern part of Hainan Island, where there was a windy area with wind speed reaching 35m/s, and the wind direction was primarily southeasterly. The

rainfall area and intensity remained essentially unchanged after Typhoon Lionrock made landfall (Figure 9(b)), but the difference is that as the typhoon continued westward and gradually moved inland towards Hainan Island, the windy area on the sea surface of northeast Hainan Island also gradually approached the northeast of Hainan Island and the eastern part of Qiongzhou Strait (Figure 9(b)). By 6:32 a.m. on the 9th, Typhoon Lionrock abruptly folded northward, and the rainfall area also moved northward, primarily in the northwestern and western areas of Hainan Island, and the intensity remained moderate to heavy, but rain in the eastern areas of Hainan Island tended to weaken; as shown in Figure 9(c), the right typhoon structure began to gradually loosen. The rainfall fallout region had moved farther north out to sea by 11:01 a.m., and the intensity had also lessened, while the overall typhoon structure was not as tight as the previous structure (Figure 9(d)). When combined with Figure 10(c), the windy area on the northeastern part of Hainan Island narrowed and moved northward to the eastern part of the Leizhou Peninsula, and the wind speed in most of Hainan Island was basically below 20m/s; only the wind speed in the western part of Hainan Island was still around 20m/s, and the wind direction changed to westerly wind, indicating that the typhoon was moving northward continuously.

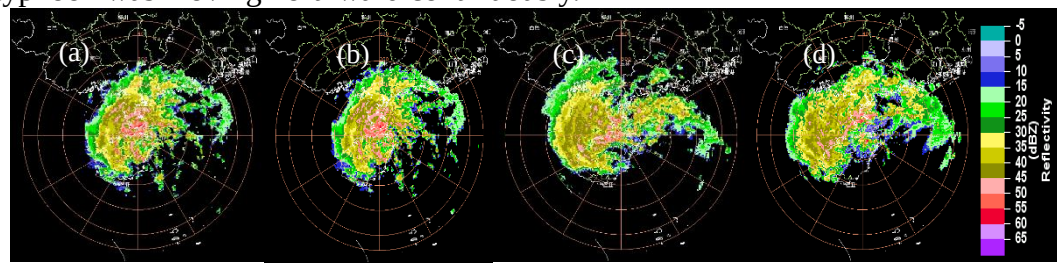


Figure 9: Grouped radar reflectance of Haikou before and after the landfall of Typhoon Lionrock and during its northward folding (a) 22:35 on October 8; (b) 22:41 on October 8; (c) 06:32 on October 9; (d) 11:01 on October 9

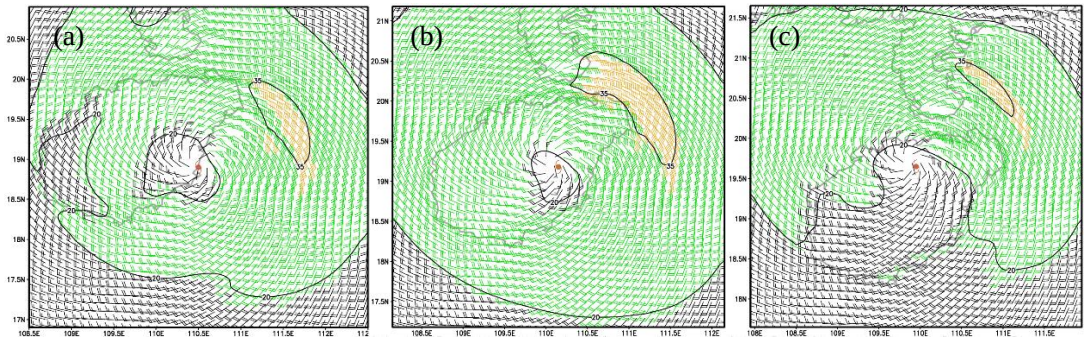


Figure 10: Map of MTCSWA wind field before and after the landfall of Typhoon Lionrock and at the time of northward folding (a) 20:00 on October 8; (b) 23:00 on October 8; (c) 05:00 on October 9

## 6. Conclusion

The storm processes of two typhoons impacting Hainan Island were compared and evaluated using a range of detection data, both conventional and unconventional, and the following results were reached.

(1) Typhoon Lionrock formed offshore and progressed slowly, bringing a huge storm process to Hainan Island and western Guangdong, along with continuous water vapor replenishment and cold air southward.

(2) PWV, FY-2G infrared cloud top brightness temperature (TBB), and vertical velocity of wind

profiler radar can accurately indicate the cloud and rain occurrence area, indicating that the atmospheric column over the atmosphere is accumulating and consuming energy, i.e., it has a certain predictive effect on precipitation development, occurrence, and end, and has a good correspondence with precipitation intensity.

(3) The horizontal wind field of the wind profiler radar and the MTCSWA wind field map can accurately indicate the typhoon's movement and the high wind area. The typhoons have gradually moved away from the sea mouth as the horizontal wind field of wind profiler radar shows the wind direction changing from southeasterly to easterly; when the wind direction is southerly, the typhoons are moving northward.

(4) The satellite cloud map and radar data revealed that Typhoon Lionrock's overall structure was loose, and the active monsoon in the South China Sea caused tropical convective clouds in the peripheral circulation to remain active, resulting in several heavy rainfall areas.

## Acknowledgments

This work was part of the Program on National Science Foundation of Hainan funded under the Hainan Provincial Department of Science and Technology, grant number 420QN373. The authors are grateful to all study participants.

## References

*[1] Lin Q. M., Chen Y. Z., Chen Y. Q., et al. Application of two kinds of unconventional detection data in weather forecast. Meteorological Science and Technology, 2012, 40 (3): 417-422.*

*[2] Tian W., Wu L.G., Liu Q. Y., et al. Evaluation of tropical cyclone surface wind analysis in East China Sea with NOAA/NESDIS multiplatform. Journal of Tropical Meteorology, 2016, 32 (1): 63-72.*

*[3] Yu X. J., Tang Y. L., Yu Z. X., et al. Characteristics of precipitable water vapor over the Tianshan Mountains based on GPS observations. Meteor Mon, 2019, 45 (12): 1691-1699 (in Chinese).*

*[4] Luo H. Y., Yang H. L., Lu Chao, et al. Comparative Analysis of Wind Speed Observation by Shenzhen Wind Profiler Radar and Meteorological Gradient Tower. Guangdong Meteorology, 2017, 39 (6): 72-76.*

*[5] Park S Y, Wan Q L, Ding W Y, et al. Impact of wind profiler data assimilation on wind field assessment over coastal areas. Asian Journal of Atmosphere Environ, 2010, 4 (3): 198-210.*

*[6] Liu S. Y., Zheng Y. G., Tao Z. Y. The analysis of the relationship between pulse of LLJ and heavy rain using wind profiler data. Journal of Tropical Meteorology, 2003, 19 (3): 285-290.*

*[7] Zhou X. Y. Structural characteristics of the low-level wind field of the landing typhoons "Swan" and "Jujue" revealed by the multi-point observation network of the wind profiler. Chinese Academy of Meteorological Sciences, 2011.*

*[8] Gou A. N., Wu C. H. Wang Y.J., et al. Meso and small-scale characteristics of heavy rain during Meiyu period in Hubei based on wind profiler radar. Journal of Arid Meteorology, 2022, 40 (1): 84-94, DOI: 10.1175/j.issn. 1006-7639 (2022)-01-0084.*

*[9] Pan C J, Reddy K K, Lai H C, et al. Wind profiler observations on orographic effects of typhoon wind structure modification over Taiwan (120.38 °E, 22.6 °N). Annales Geophysicae, 2010, 28 (1): 141-147.*

*[10] Guo J., Li G. P., Huang W. S., et al. Characteristics of GPS-retrieved precipitation water vapor in different precipitation types. Advances in Water Science, 2009, 20 (6): 763-768.*

*[11] Fu Q. Q., Li J., Zhang Y. Preliminary application of GPS/MET data on the severe convective weather process in Jiangxi. Meteorology and Disaster Reduction Research, 2011, 34 (3): 36-40.*

*[12] Chen X. L. Study on the operation and application of the ground-based GPS in Hebei. Lanzhou University, 2007.*

*[13] Pan W. H., Yu Y. J., Luo Y. Y., et al. Analysis of Spatio-temporal distribution characteristics of atmospheric precipitable resources over Fujian based on ground-based GPS Data. Journal of Arid Meteorology, 2021, 39(4): 577-584, DOI: 10.11755/j.issn. 1006-7639(2021)-04-0577.*

*[14] Xu A. H., Ying D. M., Huang Z. H. Comparative Analysis on Doppler Weather Radar Products of two Kinds of Severe Convections in Jiangxi Province. Meteorology and Disaster Reduction Research, 2007, 30 (2): 23-27.*

*[15] Ying D. M., Xu A. H., Peng J. H., et al. Analysis of a Supercell from Doppler Weather Radar Product. Meteorology and Disaster Reduction Research, 2008, 31 (4): 13-17.*

*[16] Ren X. G., Xiao T. G., Tang Z. Y. Analysis on the Doppler radar characteristics of a tornado in Xuzhou on August*

*2018. Journal of the Meteorological Sciences, 2021, 41 (2): 221-227.*
*[17] Diao X. G., Meng X. G., Zhang L., et al. Analysis of microscale vortex signature and early warning capability of tornadoes in the circulations of Typhoon YAGI and RUMBIA. Journal of Marine Meteorology, 2019, 39 (3): 19-28. DOI: 10.19513/j.cnki.issn2096-3599.2019.03.003. (in Chinese)*
*[18] Chen Z. G., Li H. Y., Xiao L. S., et al. Contrastive analysis of two intense typhoon-tornado cases with synoptic and doppler weather radar data. Journal of the Meteorological Sciences, 2021, 41 (1): 99-107.*
*[19] H. F. S., Xiao J. J., Zheng J. X., et al. On the spatiotemporal distribution of short-range intense rain of Heyuan and analysis of its radar echo characteristics. Guangdong Meteorology, 2020, 42 (6): 35-43.*
*[20] Knaff J A, DeMaria M. 2010. NOAA/NESDIS multiplatform tropical cyclone surface wind analysis. Fort Collins, Colorado: NESDIS/STAR.*
*[21] Chen K. X., Chen G. H., Xiang C. Y., et al. Statistical characteristics of wind field structures of tropical cyclones over the Western North Pacific based on MTCSWA Data. Climatic and Environmental Research (in Chinese), 2020, 25 (6): 588-600. DOI: 10.3878/j.issn.1006-9585.2020.19122.*
*[22] Xiang C. Y., Wu L. G., Tian W., et al. Applications of MTCSWA data to the characteristics analysis of tropical cyclone structure. 2016, 42 (11): 1315-1324.*
*[23] Ying M, Zhang W, Yu H, et al. An overview of the China Meteorological administration tropical cyclone data base. Journal of Atmospheric and Oceanic Technology, 2014, 31 (2): 287-301.*
*[24] Yu H. X., Zhang X. C. Application of Brightness Temperature (TBB) in Tropical Cyclone Research. China Science and Technology Information, 2009 (23): 26-27.*
*[25] Zhang X. W., Luo Z. X. Analysis of the reasons and characteristics of typhoon "Phoenix" for a long time. China Science and Technology Information, 2009 (10): 38-42.*
*[26] Chen J., Xu B., Zheng J., et al. Application of unconventional observation data on the analysis of warm area rainstorm happened in Jiangxi. Meteorology and disaster reduction research, 2015, 38 (4): 20-29.*
*[27] Fei S., Yang L., Wang G. Q., et al. Research on data credibility of wind profiler radar product. Journal of the Meteorological Sciences, 2020, 40 (4): 527-533.*
*[28] Shi C. X., Dai L.Q., Cheng H. T., et al. Application of wind profiler data in analysis of the visit by Typhoon Dianmu. Guangdong Meteorology, 2019, 41 (5): 27-30.*